Research Article | Vol. 32, No. 7 / 25 Mar 2024 / Optics Express 11010
Optics EXPRESS

Passive magnetic-free broadband optical isolator based on unidirectional self-induced transparency

HAODONG WU,[1] JIANGSHAN TANG,[1] MINGYUAN CHEN,[1] MIN XIAO,[2,3] YANQING LU,[1] KEYU XIA,[1,4,7] AND FRANCO NORI[5,6,8]

[1]College of Engineering and Applied Sciences, and National Laboratory of Solid State Microstructures, Nanjing University, Nanjing 210023, China
[2]School of Physics, Nanjing University, Nanjing 210023, China
[3]Department of Physics, University of Arkansas, Fayetteville, Arkansas 72701, USA
[4]Shishan Laboratory, Suzhou Campus of Nanjing University, Suzhou 215000, China
[5]Quantum Computing Center, Cluster for Pioneering Research, RIKEN, Wako-shi, Saitama 351-0198, Japan
[6]Physics Department, The University of Michigan, Ann Arbor, Michigan 48109-1040, USA
[7]keyu.xia@nju.edu.cn
[8]fnori@riken.jp
https://cwqed.nju.edu.cn

Abstract: Achieving a broadband nonreciprocal device without gain and any external bias is very challenging and highly desirable for modern photonic technologies and quantum networks. Here we theoretically propose a passive and magnetic-free all-optical isolator for a femtosecond laser pulse by exploiting a new mechanism of unidirectional self-induced transparency, obtained with a nonlinear medium followed by a normal absorbing medium at one side. The transmission contrast between the forward and backward directions can reach 14.3 dB for a $2\pi - 5$ fs laser pulse. The 20 dB bandwidth is about 56 nm, already comparable with a magneto-optical isolator. This work provides a new mechanism which may benefit non-magnetic isolation of ultrashort laser pulses.

1. Introduction

Nonreciprocal optical devices (NRODs), such as optical isolators and circulators, enforcing unidirectional light propagation, have become key components for modern photonic applications [1–4], quantum information processing [5–9], enhancing quantum sensing [10] and even nanofabrication of optical crystals [11]. NRODs need to break the electromagnetic time-reversal symmetry. A standard approach to implement NRODs is based on the Faraday effect using a DC magnetic bias in a magneto-optical material [12]. However, a magneto-optical system is typically incompatible with integrated photonic technologies, introduces large loss to the signal, and requires a strong magnetic field. A nonmagnetic NROD is desired for magnetically sensitive applications and integrated photonics.

Various schemes for magnetic-free nonreciprocity have been proposed and demonstrated by using spatiotemporal modulation [13–17], nonlinear resonator modes [18–20], quantum nonlinearity [21–23], nonlinearity in a parity-time-symmetry-broken system [24–27], photon-phonon coupling [28–33], moving lattice [34,35], spinning resonators [36–38], wave-mixing processes in nonlinear media [39–42], chiral quantum optical systems [30,43–57], chiral valley systems [58], reservoir engineering [59] and unidirectional quantum squeezing of microring resonator modes [60,61]. In addition, phononic and microwave nonreciprocity have been reported and have their own applications [62–66]. Meanwhile, these approaches require high-quality

#507019 https://doi.org/10.1364/OE.507019
Journal © 2024 Received 27 Sep 2023; revised 13 Feb 2024; accepted 27 Feb 2024; published 12 Mar 2024

Optics EXPRESS

cavities to enhance the light-matter interaction or narrow-band auxiliary systems, such as alkali atoms or mechanical modes. As a result, their nonreciprocal bandwidth is strongly limited.

Nonlinearity-based NRODs have attracted significant attention because they are compatible with integrated photonics and can be obtained in the absence of an external bias. Nevertheless, dynamic reciprocity imposes fundamental constraint to their practical applications [67]. The chiral Kerr nonlinearity can tackle the problem of dynamic reciprocity [50,68–70]. However, nonlinear NRODs often require nonlinear resonators, theoretically which have a very limited bandwidth.

In this work, we propose a passive magnetic-free optical isolator for an ultrashort laser pulse by using a nonlinear medium with asymmetric inputs. This magnetic-free isolator can enable unidirectional propagation of a 5 fs laser pulse. A 56 nm bandwidth can be obtained for 20 dB isolation.

2. System and model

Our proposed optical isolator consists of a one-dimensional(1D) two-level atom (TLA) medium and a normal-absorpting (NA) medium, as schematically depicted in Fig. 1. The TLA medium is followed by a NA medium in the right-hand end. The NA medium causes absorption to a laser field. For simplicity, we consider the TLA and NA media to be surrounded by air, for the theoretical analysis. In practice, the TLA medium can be a semiconductor [71,72], an ensemble of atoms [73], or semiconductor quantum dots doped in an optical material [74–77].

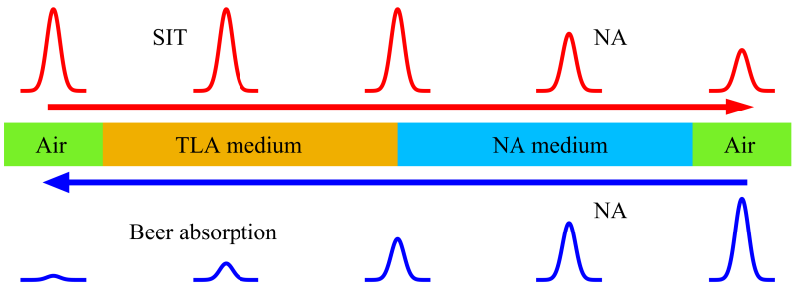

Fig. 1. Schematic of the passive magnetic-free optical isolator consisting of a TLA medium and a NA medium. The forward-moving femtosecond laser pulse first passes the TLA medium without light loss due to the self-induced transparency (SIT) and then is partially absorbed by the NA medium (red pulses). The backward-moving pulse (blue pulses) first decays to an area smaller than π due to the absorption in the NA medium, and then is further strongly absorbed in the TLA medium according to the Beer's law [78].

We use a standard two-level model for the TLA medium. The transition between the ground state $|g\rangle$ and the excited state $|e\rangle$ of the TLA system has a resonance frequency ω_0 and a vector electronic dipole moment $\vec{d}$ with amplitude d. The population relaxation time and the decoherence time are T_1 and T_2, respectively.

We assume that a laser field is polarized along $\vec{d}$ with angular frequency ω_L. At position z and time t, its envelope is $\tilde{E}_x(z,t)$. The envelope area of a laser pulse is defined as [78]

$$A = \frac{d}{\hbar}\int_{-\infty}^{\infty}\tilde{E}_x(t)dt\ . \tag{1}$$

The pulse energy is calculated as

$$U(z) = \frac{1}{2}\varepsilon_0\int_{-\infty}^{\infty}\tilde{E}_x^2(z,t)dt\ , \tag{2}$$

with ε_0 being the vacuum permittivity.

Optics EXPRESS

The propagation of a short laser pulse with a duration $\tau_p \ll T_1, T_2$ in a TLA medium is crucially dependent on its area A [78]. Due to the strong nonlinear interaction, an ultrashort laser pulse with area $A = 2\pi$ and resonance frequency $\omega_L = \omega_0$ drives a full Rabi oscillation of the TLA medium. This process takes place much faster than the relaxation and decoherence rates. During propagation, the first-half part of the 2π laser pulse coherently transfers energy to atoms and completely inverts the atomic population. Then, the atoms coherently return back the energy to the laser pulse after being "pulled" back to the ground state by the second-half part. Thus, the 2π laser pulse can propagate as the nonlinear medium is transparent and maintain its area 2π. In this case, the laser pulse can be considered as a light soliton with very small energy loss. This SIT phenomenon has been demonstrated in various experiments [79–81] and by numerical simulations based on the Maxwell-Bloch equations [82–90]. When $\pi<A<2\pi$, the pulse will quickly evolve to a 2π pulse at the expense of losing some energy. If $A<\pi$, the pulse will be strongly absorbed. Its total intensity or energy reduces exponentially according to Beer's law [78]. A π pulse is unstable and will decay during propagation.

The key idea of our isolator can be explained as follows. When ultrashort pulse with area $A \sim 2\pi$ enters the device from the left end (to the TLA medium) in the forward case, the TLA medium is mostly transparent because of the SIT. Then, the pulse leaves the device after a small absorption and outer the NA medium. This forward transmission can be high. In contrast, in the backward case, the pulse first inputs to the right end of the NA medium; it is partially absorbed by the NA medium and then suffers a Beer-law decay in intensity (energy) inside the TLA medium. Thus, the asymmetric arrangement of the NA medium causes unidirectional SIT, indicating a strong magnetic-free optical nonreciprocity.

Now we model the propagation of the laser pulse $E_x(t)$ in the TLA medium with the Maxwell-Bloch coupling equations. The TLA-field interaction can be described by the Hamiltonian without the rotating-wave approximation and the slowly varying envelope approximation as

$$H = \begin{pmatrix} \hbar\omega_0/2 & dE_x(t) \\ dE_x(t) & -\hbar\omega_0/2 \end{pmatrix}. \tag{3}$$

We consider a 1D continuous TLA medium with a number density N_a. The Maxwell's equations for the electric field E_x and the magnetic field B_y take the form

$$\partial_t B_y = -\partial_z E_x \,, \tag{4a}$$

$$\partial_t D_x = -\frac{1}{\mu_0}\partial_z B_y \,, \tag{4b}$$

where μ_0 is the magnetic permeability in the vacuum. The nonlinear response of the TLA medium is taken into account via the relation $D_x = \varepsilon_0 E_x + P_x$, where the macroscopic polarization $P_x = -N_a d u$ is connected with the off-diagonal density matrix element $\langle e|\rho|g\rangle = (u + iv)/2$. P_x can be solved by the Bloch equations

$$\partial_t u = -\frac{1}{T_2}u + \omega_0 v \,, \tag{5a}$$

$$\partial_t v = -\omega_0 u - \frac{1}{T_2}v + 2\frac{dE_x}{\hbar}w \,, \tag{5b}$$

$$\partial_t w = -2\frac{dE_x}{\hbar}w - \frac{1}{T_1}(w - w_0) \,, \tag{5c}$$

where w is the population difference between the excited state and the ground state. Note that u, v, and w satisfy the relationship $u^2 + v^2 + w^2 = 1$. This model can reproduce well experimental results [78,91] and has been widely used to study the time evolution of a femtosecond laser pulse in a nonlinear medium [92,93].

Optics EXPRESS

3. Numerical method

We employ the standard finite-difference time-domain method (FDTD) and the fourth-order Runge-Kutta method to solve the Maxwell-Bloch coupling equations [84,87–89]. The Mur absorbing boundary condition is used to avoid the reflection off the truncated boundary of the FDTD simulation domain [94]. A source laser pulse is introduced to the air region at $z_\mathrm{f} = 15\,\mu\mathrm{m}$ in the forward case and at $z_\mathrm{b} = 225\,\mu\mathrm{m}$ in the backward case. It is assumed to be a sech function defined as $E_x(t) = \tilde{E}_x(t,\tau)\sin(\omega_\mathrm{L}(t-\tau))$ with $\tilde{E}_x(t,\tau) = E_0\mathrm{sech}[1.76(t-\tau)/\tau_p]$, where E_0 is the amplitude. The delay τ is much larger than duration τ_p to ensure that the electric field is negligible at $t = 0$. Specifically, $\tau{>}4\tau_p$. The area of the input pulse is $A_0 = dE_0\tau_p\pi/1.76\hbar$.

Now we specify the TLA medium and the NA medium. The TLA medium is set at $30 \le z \le 120\,\mu\mathrm{m}$ and the NA medium at $120 \le z \le 210\,\mu\mathrm{m}$. The medium in the rest regions is air. The time-dependent transmitted pulses are retrieved at $z = 15\,\mu\mathrm{m}$ in the backward case and at $z = 225\,\mu\mathrm{m}$ in the forward case. The NA medium causes a decay of 2.93 dB in the total field energy. We refer to Ref [86–90,95] and choose the atomic parameters: $N_a = 3\times10^{19}\,\mathrm{cm}^{-3}$, $\omega_0 = 2.3\times10^{15}\,\mathrm{Hz}$ ($\lambda_0 = 820\,\mathrm{nm}$), $d = 2\times10^{-29}\,\mathrm{C\cdot m}$, $T_1 = 0.5\,\mathrm{ps}$ and $T_2 = 0.25\,\mathrm{ps}$. The TLA medium is initialized in the ground state such that $u = 0$, $v = 0$, and $w = -1$ at $t = 0$.

Without loss of generality, we adopt the typical duration $\tau_p = 5\,\mathrm{fs}$ for a resonant femtosecond laser pulse ($\omega_\mathrm{L} = \omega_0$), spanning a 200 THz bandwidth. Such ultrashort pules are well available [96–98]. For $\tau_p = 5\,\mathrm{fs}$, the pulse area can reach $A_0 = 2\pi$ when $E_0 \approx 3.7{\times}10^9\,\mathrm{V/m}$, yielding a peak Rabi frequency $\Omega_0 = 0.7\,\mathrm{fs}^{-1}$, which is much large than the atomic decoherence and relaxation rates. Thus the process is coherent. We are interested in a laser pulse with $A_0{<}3\pi$, corresponding to a peak field intensity less than $4\times10^{12}\,\mathrm{W/cm}^2$. For such laser intensity, simulation of the Maxwell-Bloch equations with the two-level system can reproduce well experimental results [82].

We evaluate the performance of the optical isolator by comparing energies of the input and transmitted laser fields. The forward and backward transmissions are calculated as

$$\mathscr{T}_\mathrm{f} = -10\log_{10}[U(z = 210\,\mu\mathrm{m})/U(z = 30\,\mu\mathrm{m})]\,, \tag{6a}$$

$$\mathscr{T}_\mathrm{b} = -10\log_{10}[U(z = 30\,\mu\mathrm{m})/U(z = 210\,\mu\mathrm{m})]\,. \tag{6b}$$

We truncate the integral time limits because the energy of the laser pulses outside the limits is negligible. The isolation contrast is defined as $\eta = -10\log_{10}(\mathscr{T}_\mathrm{f}/\mathscr{T}_\mathrm{b})$.

4. Numerical results

We first investigate the propagation of a 2π laser pulse excited by the source at either z_f or z_b, respectively. The initial energies of both input laser pulses are $U_0 = 346.6\,\mathrm{nJ}$. The nonreciprocal propagation can be seen from Fig. 2. In the forward case, see Fig. 2(a), the laser pulse enters the TLA medium at about $t = 50\,\mathrm{fs}$ with a negligible reflection and leaves at $t = 350\,\mathrm{fs}$ with the unchanged pulse shape. The laser energy decays to 79.1% of the initial energy U_0 due to the fast atomic dissipation. After going through the nonlinear medium, the energy of the pulse further decays by about 2.93 dB due to the absorption of the NA medium. The laser pulse transmitted through the device retain 40.3% of U_0, about 139.7 nJ yielding $\mathscr{T}_\mathrm{f} = 40.3\%$. Nevertheless, the pulse keeps its shape unchanged after passing through the isolator. In the backward case, see Fig. 2(b), the laser pulse with the same area is excited by the source at z_b. In stark contrast, the backward-moving laser pulse is first absorbed to an area well smaller than 2π, corresponding to 50.9% of the initial energy, and then enters the TLA medium at $t = 350\,\mathrm{fs}$. The pulse area remains about 1.4π. During propagation, the pulse quickly splits into two parts, a fast-decaying strong pulse and a slowly-decaying weak one with an oscillating envelope. According to Beer's law, the TLA medium strongly absorbs the main pulse but leaves the negligibly small oscillating one, corresponding to a 2π pulse but with a smaller energy decay scale with respect to the Beer's law. When the laser field passes through the TLA medium, only 1.49% of the initial energy of

Optics EXPRESS

the pulse, about 5.16 nJ corresponding to $\mathscr{T}_b = 1.49\%$, remains. Most energy of the backward pulse, 341.44 nJ, is blocked by the isolator.

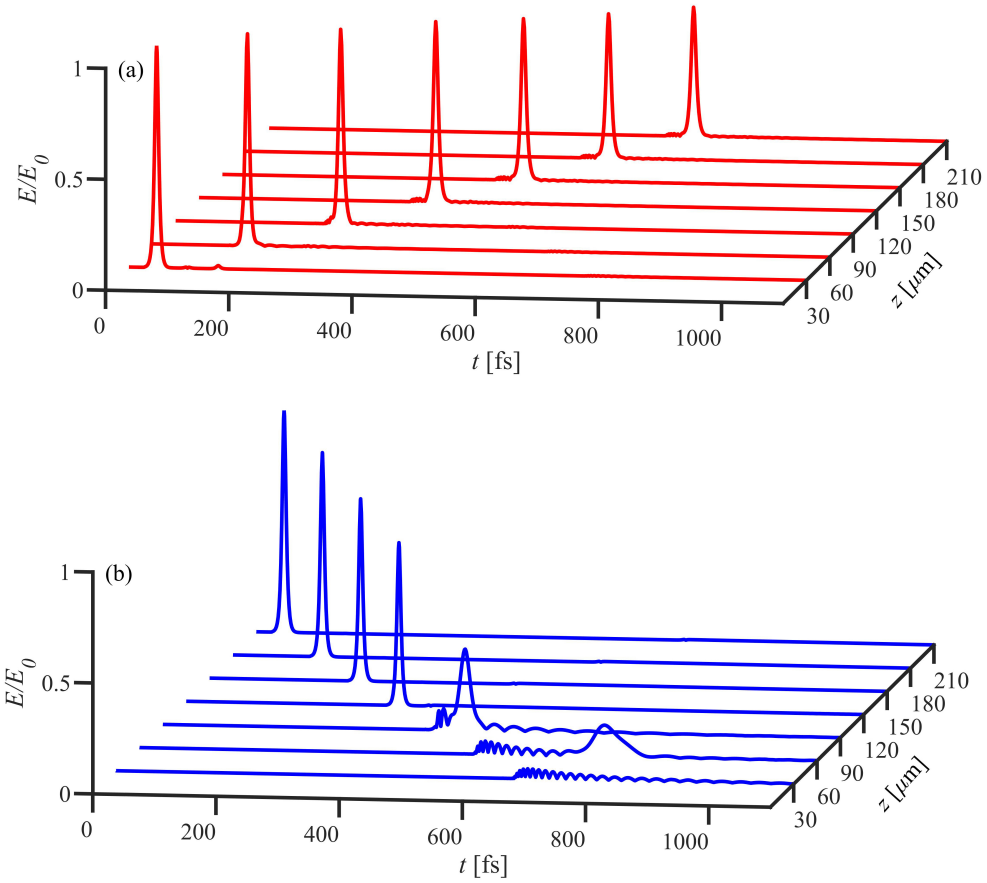

Fig. 2. Evolution of a 2π femtosecond laser pulse with $\tau_p = 5$ fs in the forward case (a) and the backward case (b).

This nonreciprocal energy evolution of the laser pulses due to the unidirectional SIT during propagation is clearly shown in Fig. 3. Our magnetic-free isolator already achieves an isolation contrast of 14.3 dB for an entire 5 fs laser pulse at the cost of a 3.95 dB insertion loss. The insertion loss in the forward case dominantly results from the absorption in the NA medium. Therefore, our theoretically proposed optical isolator can enable nonreciprocal propagation of a femtosecond laser pulse spanning over 200 THz. The discrepancy between the energy evolution (simulations) and an exponential decay (fitting) in the TLA medium is due to the slow-decaying and envelope-oscillating 2π pulse, which includes a small fraction of the total energy.

By simulating the propagation of an ultrashort laser pulse and observing the pulse field, we evaluate the nonreciprocal spectral response of the isolator. With the spectral response, we can find the limit to the duration of the laser pulse for high-performance isolation. Here, the transmission spectra and the isolation contrast versus the frequency (wavelength) are evaluated with a 5 fs laser pulse. The pulse spectra are obtained by the Fourier transform of the corresponding fields. The spectra are normalized with respect to the peak value of the input pulse spectrum. We take the time when the laser field disappears as the lower and upper temporal boundaries of the Fourier transform. As shown in Fig. 4(a), after transmitting the optical isolator, the forward-moving

Optics EXPRESS

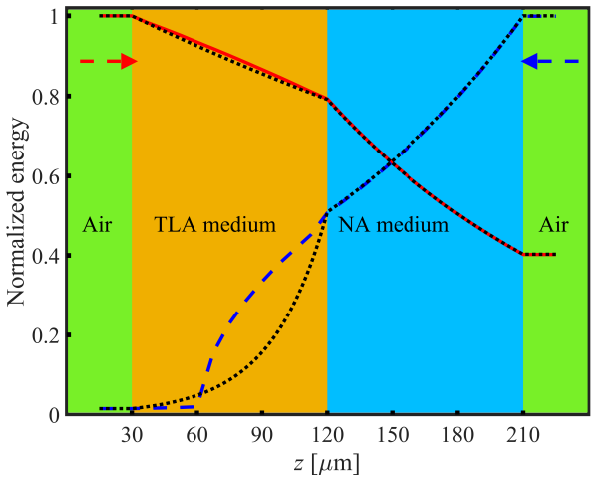

Fig. 3. Energy evolution of the forward- (red curve) and backward-moving (blue cuve) laser pulses. Dotted curves are fits with exponential decays. Red and blue arrows indicate the forward and backward transmission directions.

laser pulse retains a spectral profile similar to the input pulse, whereas a deep dip appears in the spectral center of the backward-moving pulse due to the strong Beer-law absorption of the nonlinear medium. The isolation contrast around the dip is shown in Fig. 4(b). We obtain a maximum contrast 30.5 dB at ω_L and a nonreciprocal bandwidth of 56 nm for $\eta \geq 20$ dB. This nonreciprocal bandwidth indicates that our isolator can obtain an isolation contrast larger than 20 dB for a laser pulse with duration 22 fs$<\tau_p \ll T_1, T_2$. When the laser pulse is longer than 22 fs corresponding to the bandwidth of $\leq$ 56 nm, the isolation contrast is reduced, but it is still reasonably high, as shown in Fig. 4(b). The performance of an isolator for different pulse durations can be calculated by integration from the spectral response.

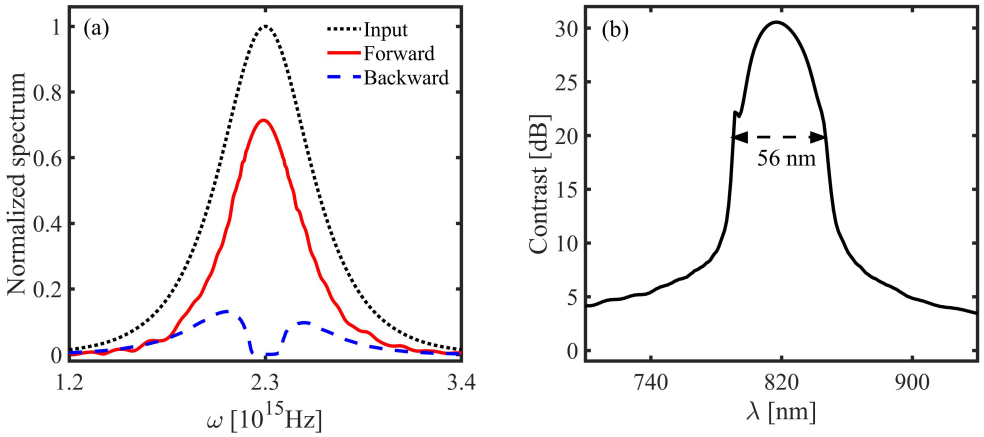

Fig. 4. (a) Spectra of the input pulse (dotted black curve), the forward-moving (solid red curve) and the backward-moving (dashed blue curve) pulses transmitted through the optical isolator. (b) Isolation contrast versus the wavelength.

The isolation contrast can be improved to a much higher value by using a TLA medium long enough, because the decay of the forward-moving laser pulse is mostly determined by the NA medium and thus fixed, while the backward-moving laser pulse with an area $A<\pi$ initially in

Optics EXPRESS

the TLA medium can be completely absorbed. Here, we choose a 90 μm nonlinear medium for demonstrating the concept of our isolator and remaining the reasonably high forward transmission. A 5 fs pulse is used as an example to find the nonreciprocal band covering the nonreciprocal window. Using an ultrashort pulse with different duration will obtain a similar result.

The transmission and isolation contrast versus the area of the input laser pulse are shown in Fig. 5. Here, the isolation contrast is calculated for a whole femtosecond laser pulse. When $2\pi<A<3\pi$, the forward transmission is stable and high, larger than 40%. We obtain the maximal isolation contrast 16.9 dB when $A = 2.15\pi$. However, when $A>2.15\pi$, the backward transmission quickly increases to a high level. According to the "area theorem" [78], if the area of a femtosecond laser pulse is less than π when it enters the TLA medium, its energy can be completely absorbed in the TLA medium. However, when $A>2\pi$, the laser pulse will split into multi daughter pulses although the daughter pulses are under the SIT. To guarantee a high and shape-maintaining transmission in the forward case, the pulse area when entering the TLA medium needs to be no more than 2π to avoid splitting. Thus, the nonreciprocal energy range is narrow. Note that there is a small reflection caused by the air-medium interface. We can attain high-performance isolation for $1.71\pi<A<2.25\pi$.

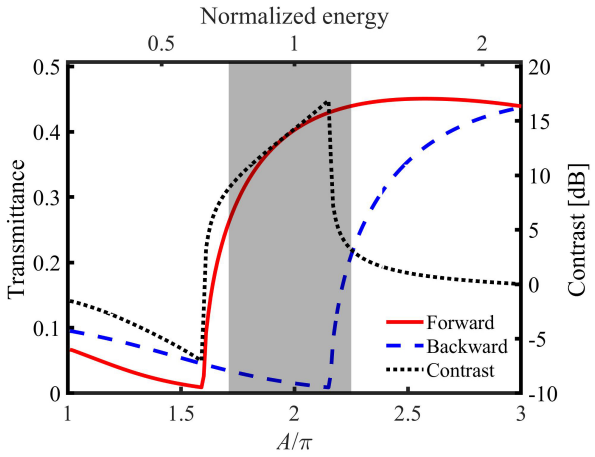

Fig. 5. Transmission and isolation contrast of the optical isolator versus the pulse area A and energy for a 5 fs laser pulse.

The dynamic nonreciprocity is also obtained when the two laser pulses simultaneously propagate in the TLA medium along opposite directions. We study the two counter-propagating 2π laser pulses as an example. To allow the two laser pulses to meet in the medium, we input the backward-moving pulse about 300 fs earlier than the forward-moving pulse. Figure 6 shows the normalized electric fields of the pulses and the population inversion w. When the forward- and backward-moving pulses meet, the population inversion w oscillates quickly. However, the two laser pulses can pass each other without observable interference as two light solitons. The transmission of the backward-moving pulse is much smaller than the forward-moving pulse. These results confirm that *our proposed optical isolator displays dynamic nonreciprocity*.

Optics EXPRESS

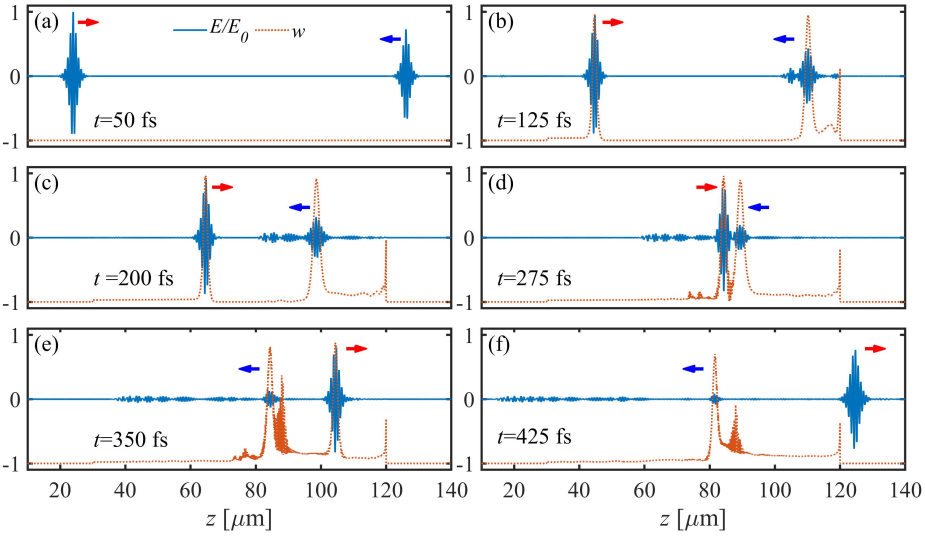

Fig. 6. Field distribution of a 5 fs laser pulse (blue curves) in the TLA medium and the population difference w (brown curves) at different times. Red and blue arrows indicate the forward and backward moving directions.

5. Conclusion and discussion

In summary, we have shown unidirectional SIT as a novel mechanism for obtaining a passive magnetic-free optical isolator. This isolator displays dynamic nonreciprocity over an broad bandwith comparable with a magneto-optical nonreciprocal device. This broadband nonreciprocial device has the potential to be integrated on a chip in a semiconductor platform and thus can boost applications of integrated photonics and femtosecond lasers.

This work proposes a new approache for magnetic-free optical isolation of few- fs laser pulses. With the progress of integrated photonics and microresonators, a train of ultrashort laser solitons as frequency combs can be generated on a chip platform [99–101]. Generation of optical frequency combs from a microresonator is extremely sensitive to noise and field backscattering. Thus, this work may provide an approach to integrate a non-magnetic isolator for future applications in isolation of backscattering from optical frequency combs. This function may boost the applications of an on-chip frequency combs.

Although conventional isolators based on the magneto-optical effect can protect an ultrashort laser, it is subject to dispersion because the Faraday rotation of polarization of light is proportional to the inverse of the light wavelength. This strong dispersion limits the high-performance isolation bandwidth and causes a large insertion loss. Our scheme already shows strong isolation for a 5 fs laser pulse. It may provide a dispersion-immune method for protecting fs lasers from backscattering of ultrashort laser pulses.

The SIT has been observed in various media, such as Ruby [102], vapors of alkali atoms [73], Rydberg atoms [103], molecular gases [104], semiconductors [71,72] and semiconductor quantum dots [74–76,105]. Semiconductors possess short relaxation times and comparatively high transition dipole moments. Semiconductor quantum dots can be artificial TLAs with high dipole moments [76,105]. The conditions required by our method can be satisfied with semiconductors [74,75]. Thus, an on-chip optical isolator based on unidirectional SIT can be integrated on a semiconductor platform.

Note that SIT of a few-cycle rf pulse has been experimentally observed in Rubidium atoms and is reproduced by solving the Bloch equation [91]. Therefore, the concept of our optical isolator

Optics EXPRESS

can be extended to the rf regime. If a TLA medium with small dissipation is available [103], our method can also isolate the reflection of a long light pulse.

Funding. the Quantum Leap Flagship Program (Q-LEAP); Office of Naval Research (N62909-23-1-2074); Asian Office of Aerospace Research and Development (FA2386-20-1-4069); Moonshot Research and Development Program (JPMJMS2061); Japan Science and Technology Agency; Nippon Telegraph and Telephone; Innovative Team of Jiangsu Province (JSSCTD202138); Fundamental Research Funds for the Central Universities (021314380095); National Natural Science Foundation of China (92365107); National Key Research and Development Program of China (2019YFA0308700, 2019YFA0308704).

Disclosures. The authors declare no conflicts of interest.

Data availability. Data underlying the results presented in this paper are not publicly available at this time but may be obtained from the authors upon reasonable request.

References

1. G. Millot, S. Pitois, M. Yan, *et al.*, "Frequency-agile dual-comb spectroscopy," Nat. Photonics **10**(1), 27–30 (2016).
2. X. Zhang, K. Kwon, J. Henriksson, *et al.*, "A large-scale microelectromechanical-systems-based silicon photonics lidar," Nature **603**(7900), 253–258 (2022).
3. J. Shin, Z. Liu, W. Bai, *et al.*, "Bioresorbable optical sensor systems for monitoring of intracranial pressure and temperature," Sci. Adv. **5**(7), eaaw1899 (2019).
4. Y.-H. Lai, M.-G. Suh, Y.-K. Lu, *et al.*, "Earth rotation measured by a chip-scale ring laser gyroscope," Nat. Photonics **14**(6), 345–349 (2020).
5. S. Daiss, S. Langenfeld, S. Welte, *et al.*, "A quantum-logic gate between distant quantum-network modules," Science **371**(6529), 614–617 (2021).
6. A. Wallucks, I. Marinković, B. Hensen, *et al.*, "A quantum memory at telecom wavelengths," Nat. Phys. **16**(7), 772–777 (2020).
7. H. J. Kimble, "The quantum internet," Nature **453**(7198), 1023–1030 (2008).
8. J. I. Cirac, P. Zoller, H. J. Kimble, *et al.*, "Quantum state transfer and entanglement distribution among distant nodes in a quantum network," Phys. Rev. Lett. **78**(16), 3221–3224 (1997).
9. T. Zhong, J. M. Kindem, J. G. Bartholomew, *et al.*, "Nanophotonic rare-earth quantum memory with optically controlled retrieval," Science **357**(6358), 1392–1395 (2017).
10. L. Bao, B. Qi, D. Dong, *et al.*, "Fundamental limits for reciprocal and nonreciprocal non-Hermitian quantum sensing," Phys. Rev. A **103**(4), 042418 (2021).
11. X. Xu, T. Wang, P. Chen, *et al.*, "Femtosecond laser writing of lithium niobate ferroelectric nanodomains," Nature **609**(7927), 496–501 (2022).
12. S.-Y. Ren, W. Yan, L.-T. Feng, *et al.*, "Single-photon nonreciprocity with an integrated magneto-optical isolator," Laser Photonics Rev. **16**(5), 2100595 (2022).
13. H. Lira, Z. Yu, S. Fan, *et al.*, "Electrically driven nonreciprocity induced by interband photonic transition on a silicon chip," Phys. Rev. Lett. **109**(3), 033901 (2012).
14. N. A. Estep, D. L. Sounas, J. Soric, *et al.*, "Magnetic-free non-reciprocity and isolation based on parametrically modulated coupled-resonator loops," Nat. Phys. **10**(12), 923–927 (2014).
15. D. L. Sounas and A. Alù, "Non-reciprocal photonics based on time modulation," Nat. Photonics **11**(12), 774–783 (2017).
16. L. D. Tzuang, K. Fang, P. Nussenzveig, *et al.*, "Non-reciprocal phase shift induced by an effective magnetic flux for light," Nat. Photonics **8**(9), 701–705 (2014).
17. H. Tian, J. Liu, A. Siddharth, *et al.*, "Magnetic-free silicon nitride integrated optical isolator," Nat. Photonics **15**(11), 828–836 (2021).
18. K. Y. Yang, J. Skarda, M. Cotrufo, *et al.*, "Inverse-designed non-reciprocal pulse router for chip-based lidar," Nat. Photonics **14**(6), 369–374 (2020).
19. L. Fan, J. Wang, L. T. Varghese, *et al.*, "An all-silicon passive optical diode," Science **335**(6067), 447–450 (2012).
20. M. Cotrufo, A. Cordaro, D. L. Sounas, *et al.*, "Passive bias-free non-reciprocal metasurfaces based on thermally nonlinear quasi-bound states in the continuum," Nat. Photonics **18**(1), 81–90 (2024).
21. P. Yang, X. Xia, H. He, *et al.*, "Realization of nonlinear optical nonreciprocity on a few-photon level based on atoms strongly coupled to an asymmetric cavity," Phys. Rev. Lett. **123**(23), 233604 (2019).
22. F. Fratini, E. Mascarenhas, L. Safari, *et al.*, "Fabry-Perot interferometer with quantum mirrors: nonlinear light transport and rectification," Phys. Rev. Lett. **113**(24), 243601 (2014).
23. G. Hétet, L. Slodička, M. Hennrich, *et al.*, "Single atom as a mirror of an optical cavity," Phys. Rev. Lett. **107**(13), 133002 (2011).
24. L. Chang, X. Jiang, S. Hua, *et al.*, "Parity-time symmetry and variable optical isolation in active-passive-coupled microresonators," Nat. Photonics **8**(7), 524–529 (2014).
25. B. Peng, Ş. K. Özdemir, F. Lei, *et al.*, "Parity-time-symmetric whispering-gallery microcavities," Nat. Phys. **10**(5), 394–398 (2014).

Optics EXPRESS

26. B. He, L. Yang, X. Jiang, *et al.*, "Transmission nonreciprocity in a mutually coupled circulating structure," Phys. Rev. Lett. **120**(20), 203904 (2018).
27. I. I. Arkhipov, A. Miranowicz, O. Di Stefano, *et al.*, "Scully-Lamb quantum laser model for parity-time-symmetric whispering-gallery microcavities: gain saturation effects and nonreciprocity," Phys. Rev. A **99**(5), 053806 (2019).
28. E. A. Kittlaus, W. M. Jones, P. T. Rakich, *et al.*, "Electrically driven acousto-optics and broadband non-reciprocity in silicon photonics," Nat. Photonics **15**(1), 43–52 (2021).
29. Z. Shen, Y.-L. Zhang, Y. Chen, *et al.*, "Experimental realization of optomechanically induced non-reciprocity," Nat. Photonics **10**(10), 657–661 (2016).
30. X.-X. Hu, Z.-B. Wang, P. Zhang, *et al.*, "Noiseless photonic non-reciprocity via optically-induced magnetization," Nat. Commun. **12**(1), 2389 (2021).
31. M. S. Kang, A. Butsch, and P. S. J. Russell, "Reconfigurable light-driven opto-acoustic isolators in photonic crystal fibre," Nat. Photonics **5**(9), 549–553 (2011).
32. D. B. Sohn, S. Kim, and G. Bahl, "Time-reversal symmetry breaking with acoustic pumping of nanophotonic circuits," Nat. Photonics **12**(2), 91–97 (2018).
33. J. Kim, M. C. Kuzyk, K. Han, *et al.*, "Non-reciprocal Brillouin scattering induced transparency," Nat. Phys. **11**(3), 275–280 (2015).
34. D.-W. Wang, H.-T. Zhou, M.-J. Guo, *et al.*, "Optical diode made from a moving photonic crystal," Phys. Rev. Lett. **110**(9), 093901 (2013).
35. S. A. R. Horsley, J.-H. Wu, M. Artoni, *et al.*, "Optical nonreciprocity of cold atom Bragg mirrors in motion," Phys. Rev. Lett. **110**(22), 223602 (2013).
36. S. Maayani, R. Dahan, Y. Kligerman, *et al.*, "Flying couplers above spinning resonators generate irreversible refraction," Nature **558**(7711), 569–572 (2018).
37. Y.-F. Jiao, S.-D. Zhang, Y.-L. Zhang, *et al.*, "Nonreciprocal optomechanical entanglement against backscattering losses," Phys. Rev. Lett. **125**(14), 143605 (2020).
38. R. Huang, A. Miranowicz, J.-Q. Liao, *et al.*, "Nonreciprocal photon blockade," Phys. Rev. Lett. **121**(15), 153601 (2018).
39. Z. Yu and S. Fan, "Complete optical isolation created by indirect interband photonic transitions," Nat. Photonics **3**(2), 91–94 (2009).
40. F. Song, Z. P. Wang, E. Z. Li, *et al.*, "Optical nonreciprocity using four-wave mixing in hot atoms," Appl. Phys. Lett. **119**(2), 024101 (2021).
41. H. Yang, S. C. Zhang, Y. P. Niu, *et al.*, "Ultra-strong nonreciprocal amplification with hot atoms," Opt. Commun. **515**(2), 128195 (2022).
42. S. Hua, J. Wen, X. Jiang, *et al.*, "Demonstration of a chip-based optical isolator with parametric amplification," Nat. Commun. **7**(1), 13657 (2016).
43. K. Xia, G. Lu, G. Lin, *et al.*, "Reversible nonmagnetic single-photon isolation using unbalanced quantum coupling," Phys. Rev. A **90**(4), 043802 (2014).
44. C. Sayrin, C. Junge, R. Mitsch, *et al.*, "Nanophotonic optical isolator controlled by the internal state of cold atoms," Phys. Rev. X **5**(4), 041036 (2015).
45. M. Scheucher, A. Hilico, E. Will, *et al.*, "Quantum optical circulator controlled by a single chirally coupled atom," Science **354**(6319), 1577–1580 (2016).
46. I. Söllner, S. Mahmoodian, S. L. Hansen, *et al.*, "Deterministic photon-emitter coupling in chiral photonic circuits," Nat. Nanotechnol. **10**(9), 775–778 (2015).
47. L. Tang, J.-S. Tang, W. Zhang, *et al.*, "On-chip chiral single-photon interface: isolation and unidirectional emission," Phys. Rev. A **99**(4), 043833 (2019).
48. J.-S. Tang, W. Nie, L. Tang, *et al.*, "Nonreciprocal single-photon band structure," Phys. Rev. Lett. **128**(20), 203602 (2022).
49. S. Zhang, Y. Hu, G. Lin, *et al.*, "Thermal-motion-induced non-reciprocal quantum optical system," Nat. Photonics **12**(12), 744–748 (2018).
50. K. Xia, F. Nori, and M. Xiao, "Cavity-free optical isolators and circulators using a chiral cross-Kerr nonlinearity," Phys. Rev. Lett. **121**(20), 203602 (2018).
51. M.-X. Dong, K.-Y. Xia, W.-H. Zhang, *et al.*, "All-optical reversible single-photon isolation at room temperature," Sci. Adv. **7**(12), eabe8924 (2021).
52. C. Liang, B. Liu, A.-N. Xu, *et al.*, "Collision-induced broadband optical nonreciprocity," Phys. Rev. Lett. **125**(12), 123901 (2020).
53. H. Wu, Y. Ruan, Z. Li, *et al.*, "Fundamental distinction of electromagnetically induced transparency and Autler-Townes splitting in breaking the time-reversal symmetry," Laser Photonics Rev. **16**(9), 2100708 (2022).
54. Wang Zhu-Bo, Zhang Yan-Lei, Hu Xin-Xin, *et al.*, "Self-induced optical non-reciprocity," arXiv, arXiv.2210.07038 (2022).
55. S. Pucher, C. Liedl, S. Jin, *et al.*, "Atomic spin-controlled non-reciprocal Raman amplification of fibre-guided light," Nat. Photonics **16**(5), 380–383 (2022).
56. L. Tang, J.-S. Tang, and K. Xia, "Chiral quantum optics and optical nonreciprocity based on susceptibility-momentum locking," Adv. Quantum Technol. **5**(8), 2200014 (2022).

Optics EXPRESS

57. W. Nie, T. Shi, F. Nori, *et al.*, "Topology-enhanced nonreciprocal scattering and photon absorption in a waveguide," Phys. Rev. Appl. **15**(4), 044041 (2021).
58. S. Guddala, Y. Kawaguchi, F. Komissarenko, *et al.*, "All-optical nonreciprocity due to valley polarization pumping in transition metal dichalcogenides," Nat. Commun. **12**(1), 3746 (2021).
59. A. Metelmann and A. A. Clerk, "Nonreciprocal photon transmission and amplification via reservoir engineering," Phys. Rev. X **5**(2), 021025 (2015).
60. L. Tang, J.-S. Tang, M. Chen, *et al.*, "Quantum squeezing induced optical nonreciprocity," Phys. Rev. Lett. **128**(8), 083604 (2022).
61. X. Guo, C.-L. Zou, H. Jung, *et al.*, "On-chip strong coupling and efficient frequency conversion between telecom and visible optical modes," Phys. Rev. Lett. **117**(12), 123902 (2016).
62. X. C. Xu, Q. Wu, H. Chen, *et al.*, "Physical observation of a robust acoustic pumping in waveguides with dynamic boundary," Phys. Rev. Lett. **125**(25), 253901 (2020).
63. X. F. Li, X. Ni, L. A. Feng, *et al.*, "Tunable unidirectional sound propagation through a sonic-crystal-based acoustic diode," Phys. Rev. Lett. **106**(8), 084301 (2011).
64. Y. P. Wang, J. W. Rao, Y. Yang, *et al.*, "Nonreciprocity and unidirectional invisibility in cavity magnonics," Phys. Rev. Lett. **123**(12), 127202 (2019).
65. P. Huang, L. Zhang, J. Zhou, *et al.*, "Nonreciprocal radio frequency transduction in a parametric mechanical artificial lattice," Phys. Rev. Lett. **117**(1), 017701 (2016).
66. D.-G. Lai, J.-F. Huang, X.-L. Yin, *et al.*, "Nonreciprocal ground-state cooling of multiple mechanical resonators," Phys. Rev. A **102**(1), 011502 (2020).
67. Y. Shi, Z. Yu, and S. Fan, "Limitations of nonlinear optical isolators due to dynamic reciprocity," Nat. Photonics **9**(6), 388–392 (2015).
68. E.-Z. Li, D.-S. Ding, Y.-C. Yu, *et al.*, "Experimental demonstration of cavity-free optical isolators and optical circulators," Phys. Rev. Res. **2**(3), 033517 (2020).
69. L. D. Bino, J. M. Silver, M. T. M. Woodley, *et al.*, "Microresonator isolators and circulators based on the intrinsic nonreciprocity of the Kerr effect," Optica **5**(3), 279–282 (2018).
70. R.-K. Pan, L. Tang, K. Xia, *et al.*, "Dynamic nonreciprocity with a Kerr nonlinear resonator," Chin. Phys. Lett. **39**(12), 124201 (2022).
71. I. A. Poluéktov, Y. M. Popov, and V. S. Roïtberg, "Self-induced transparency effect," Sov. Phys. Usp. **17**(5), 673–690 (1975).
72. Y. Wu, I. M. Piper, M. Ediger, *et al.*, "Population inversion in a single InGaAs quantum dot using the method of adiabatic rapid passage," Phys. Rev. Lett. **106**(6), 067401 (2011).
73. H. M. Gibbs and R. E. Slusher, "Sharp-line self-induced transparency," Phys. Rev. A **6**(6), 2326–2334 (1972).
74. N. C. Nielsen, T. H. zu Siederdissen, J. Kuhl, *et al.*, "Phase evolution of solitonlike optical pulses during excitonic Rabi flopping in a semiconductor," Phys. Rev. Lett. **94**(5), 057406 (2005).
75. H. Giessen, A. Knorr, S. Haas, *et al.*, "Self-induced transmission on a free exciton resonance in a semiconductor," Phys. Rev. Lett. **81**(19), 4260–4263 (1998).
76. S. Schneider, P. Borri, W. Langbein, *et al.*, "Self-induced transparency in InGaAs quantum-dot waveguides," Appl. Phys. Lett. **83**(18), 3668–3670 (2003).
77. U.-S. Kim and Y.-H. Kim, "Simultaneous trapping of two optical pulses in an atomic ensemble as stationary light pulses," Phys. Rev. Lett. **129**(9), 093601 (2022).
78. L. Allen and J. H. Eberly, *Optical resonance and two-level atoms* (Dover Publications, 1987), pp. 1–129.
79. T. Carmon, C. Anastassiou, S. Lan, *et al.*, "Observation of two-dimensional multimode solitons," Opt. Lett. **25**(15), 1113–1115 (2000).
80. D. Neshev, E. Ostrovskaya, Y. Kivshar, *et al.*, "Spatial solitons in optically induced gratings," Opt. Lett. **28**(9), 710–712 (2003).
81. C. Rotschild, M. Segev, Z. Xu, *et al.*, "Two-dimensional multipole solitons in nonlocal nonlinear media," Opt. Lett. **31**(22), 3312–3314 (2006).
82. W. E. Lamb, "Theory of an optical maser," Phys. Rev. **134**(6A), A1429–A1450 (1964).
83. S. L. McCall and E. L. Hahn, "Self-induced transparency by pulsed coherent light," Phys. Rev. Lett. **18**(21), 908–911 (1967).
84. S. Hughes, "Breakdown of the area theorem: carrier-wave Rabi flopping of femtosecond optical pulses," Phys. Rev. Lett. **81**(16), 3363–3366 (1998).
85. R. W. Ziolkowski, J. M. Arnold, and D. M. Gogny, "Ultrafast pulse interactions with two-level atoms," Phys. Rev. A **52**(4), 3082–3094 (1995).
86. K. Xia, S. Gong, C. Liu, *et al.*, "Near dipole-dipole effects on the propagation of few-cycle pulse in a dense two-level medium," Opt. Express **13**(16), 5913 (2005).
87. K. Xia, Y. Niu, C. Li, *et al.*, "Absolute phase control of spectra effects in a two-level medium driven by two-color ultrashort laser pulses," Phys. Lett. A **361**(1-2), 173–177 (2007).
88. K. Xia, Y. Niu, R. Li, *et al.*, "Transient population and polarization gratings induced by (1 + 1)-dimensional ultrashort dipole soliton," Phys. Rev. A **75**(5), 053816 (2007).
89. K. Xia, S. Gong, Y. Niu, *et al.*, "Accurate determination of the absolute phase and temporal-pulse phase of few-cycle laser pulses," Chin. Phys. **16**(2), 472–477 (2007).

Optics EXPRESS

90. X. T. Xie and M. A. Macovei, "Single-cycle gap soliton in a subwavelength structure," Phys. Rev. Lett. **104**(7), 073902 (2010).
91. H. Li, V. A. Sautenkov, Y. V. Rostovtsev, *et al.*, "Carrier-envelope phase effect on atomic excitation by few-cycle rf pulses," Phys. Rev. Lett. **104**(10), 103001 (2022).
92. W. Forysiak, J. V. Moloney, and E. M. Wright, "Nonlinear focusing of femtosecond pulses as a result of self-reflection from a saturable absorber," Opt. Lett. **22**(4), 239 (1997).
93. O. D. Mücke, T. Tritschler, M. Wegener, *et al.*, "Role of the carrier-envelope offset phase of few-cycle pulses in nonperturbative resonant nonlinear optics," Phys. Rev. Lett. **89**(12), 127401 (2002).
94. G. Mur, "Absorbing boundary conditions for the finite-difference approximation of the time-domain electromagnetic-field equations," IEEE Trans. Electron. Comput. **EMC-23**(4), 377–382 (1981).
95. V. P. Kalosha and J. Herrmann, "Formation of optical subcycle pulses and full Maxwell-Bloch solitary waves by coherent propagation effects," Phys. Rev. Lett. **83**(3), 544–547 (1999).
96. T. Brabec and F. Krausz, "Intense few-cycle laser fields: frontiers of nonlinear optics," Rev. Mod. Phys. **72**(2), 545–591 (2000).
97. A. Baltuška, Z. Wei, M. S. Pshenichnikov, *et al.*, "Optical pulse compression to 5 fs at a 1-MHz repetition rate," Opt. Lett. **22**(2), 102–104 (1997).
98. R. Ell, U. Morgner, F. X. Kärtner, *et al.*, "Generation of 5-fs pulses and octave-spanning spectra directly from a Ti:sapphire laser," Opt. Lett. **26**(6), 373–375 (2001).
99. V. Brasch, M. Geiselmann, T. Herr, *et al.*, "Photonic chip-based optical frequency comb using soliton Cherenkov radiation," Science **351**(6271), 357–360 (2016).
100. X. Yi, Q.-F. Yang, K. Y. Yang, *et al.*, "Soliton frequency comb at microwave rates in a high-Q silica microresonator," Optica **2**(12), 1078–1085 (2015).
101. Q. Guo, B. K. Gutierrez, R. Sekine, *et al.*, "Ultrafast mode-locked laser in nanophotonic lithium niobate," Science **382**(6671), 708–713 (2023).
102. I. M. Asher, "Experimental investigation of self-induced transparency and pulse delay in ruby," Phys. Rev. A **5**(1), 349–355 (1972).
103. Z. Bai, C. S. Adams, G. Huang, *et al.*, "Self-induced transparency in warm and strongly interacting Rydberg gases," Phys. Rev. Lett. **125**(26), 263605 (2020).
104. A. Zembrod and T. Gruhl, "Self-induced transparency of degenerate transitions with thermally equilibrated levels," Phys. Rev. Lett. **27**(6), 287–290 (1971).
105. G. Panzarini, U. Hohenester, and E. Molinari, "Self-induced transparency in semiconductor quantum dots," Phys. Rev. B **65**(16), 165322 (2002).